Available online at www.sciencedirect.com
SCIENCE DIRECT®
Surface Science 529 (2003) 197–203
SURFACE SCIENCE
www.elsevier.com/locate/susc

Hot carrier luminescence during porous etching of GaP under high electric field conditions

A.F. van Driel [a,*], B.P.J. Bret [b,1], D. Vanmaekelbergh [a], J.J. Kelly [a]

[a] *Debye Institute, Chemistry of Condensed Matter, Utrecht University, Princetonplein 1, 3508 TA Utrecht, The Netherlands*
[b] *Van der Waals Zeeman-Institute, University of Amsterdam, Amsterdam 1018 XE, The Netherlands*

Received 14 November 2002; accepted for publication 29 January 2003

Abstract

Electroluminescence is observed during porous etching of n-type GaP single crystals at strongly positive potential. The emission spectra, which include a supra-bandgap contribution, are markedly different from the spectra observed under optical excitation or minority carrier injection. The current density and electroluminescence intensity show a strong potential dependence and a similar hysteresis. The spectral characteristics of the luminescence suggest that both thermalised and hot charge carriers, generated by impact ionisation, are involved in light emission.

Keywords: Electron–solid interactions; Electrochemical methods; Electroluminescence; Field emission; Porous solids; Gallium phosphide

1. Introduction

Various n-type III–V semiconductors, including InP, GaAs, GaP and GaN, can be made porous by electrochemical etching [1–7]. These materials have a large refractive index and a bandgap ranging from the near infrared to the ultra-violet [8]. III–V semiconductors with pore dimensions in the 100–500 nm range are therefore very promising materials for photonic applications. It has been demonstrated that anodic etching can produce a two-dimensional array of ordered pores in InP [3]; this material, showing birefringence at wavelengths required for optical communication, can be easily integrated in opto-electronic systems. On the other hand, anodic etching of n-type GaP gives random porous networks [2]. Optimisation of the etching process has yielded the strongest known random-scattering medium for visible light to date [9]. There is evidence for Anderson localisation of light in this system [10] and anisotropic diffusion of light has been observed [11].

In view of the very interesting optical [3,7,9,10,12] and also opto-electrical properties [12,13] the mechanism of porous etching and the influence of the etching parameters on the morphology are important. Etching is generally carried out at strongly positive potentials corresponding to deep depletion [2]. Various workers have suggested that electrical breakdown leading to current flow is

* Corresponding author. Tel.: +31-302533545; fax: +31-302532403.
E-mail address: a.f.vandriel@phys.uu.nl (A.F. van Driel).
[1] Present address: MESA+ Institute, University of Twente, P.O. Box 217, 7500 AE Enschede, The Netherlands.

0039-6028/03/$ - see front matter
doi:10.1016/S0039-6028(03)00262-0

governed by the electric field of the space-charge layer. In the present work we have investigated the relationship between the current density and potential for n-type GaP under porous etching and passivating conditions in aqueous H_2SO_4 solution. We show that the dissolution current is due to field-dependent inter-band tunnelling. In addition, we have observed for the first time very characteristic light emission during the etching process.

Electroluminescence in GaP has been reported to occur both in forward-biased p–n junctions [14,15] and n-type electrodes in the presence of a hole-injecting species, i.e. a strong oxidising agent [16]. Since GaP has an indirect bandgap (at 2.24 eV [17]) band-band emission is, except for iso-electronically doped material, very inefficient. At room temperature one generally observes only sub-bandgap emission due to electron–hole recombination via defect states, e.g. donor–acceptor pairs [16]. A similar emission spectrum, consisting of a broad band with a maximum at around 1.55 eV is also observed in room-temperature photoluminescence [16] and cathodoluminescence [18]. In our experiments with anodically etching GaP we find, surprisingly, not only the sub-bandgap luminescence but also relatively strong emission at higher energies; we observe a broad band extending well above the indirect bandgap. In the present paper we describe the influence of various parameters (potential, current density and the porous layer thickness) on the intensity, current efficiency and the spectral distribution of the luminescence. We show that this striking electroluminescence originates from the area of active etching and we speculate on the mechanism.

2. Experimental

For the experiments 300 μm thick n-GaP wafers, supplied by Groupe Arnaud Electronics and Grimet Ltd., with a (1 0 0) surface orientation and a dopant density of 7×10^{17} cm^{-3} or $10–20 \times 10^{17}$ cm^{-3} were used. Pieces of approximately 6×6 mm were cut and glued on a copper plate with a conductive adhesive paste. A circular area of 0.13 cm^2 was exposed to the electrolyte by means of a Teflon sticker. Experiments were performed with the n-GaP working electrode in a three-electrode set-up, with a platinum counter electrode and a saturated calomel electrode (SCE) as reference. All experiments were performed in the dark, at room temperature in an aqueous 0.5 M H_2SO_4 solution. The potential of the GaP working electrode was controlled by an EG & G PAR 273A potentiostat, which was programmed by a computer with home-made software. Luminescence spectra were recorded with a Princeton Instruments CCD camera (liquid-nitrogen cooled, 1024×256 pixels) in combination with an Acton Pro monochromator (150 lines/mm, blazed at 500 nm).

3. Results

Fig. 1 shows a current density-time plot for the higher doped n-type GaP electrode ($10–20 \times 10^{17}$ cm^{-3}) during the first 1000 s of porous etching at a potential of 7 V. Etching of the GaP crystal starts at $t = 0$ s. In the initial stage of porous etching the current rises rapidly; it reaches a constant value of about 13 mA/cm^2 after approximately 200 s. Previous studies [2,19] have shown that etching starts at defect sites on the surface and that the pores have a diameter of around 100 nm. Here primary pores are formed from which multiple branching occurs, resulting in an increased active etching

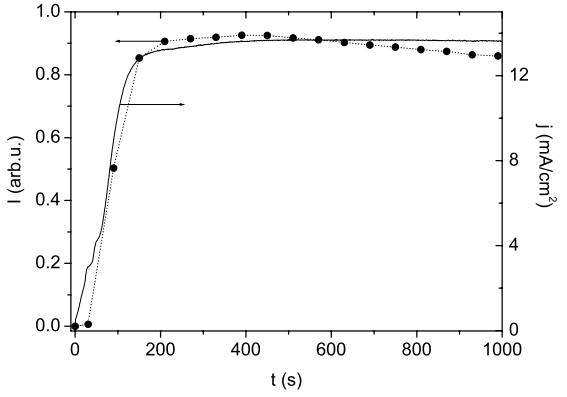

Fig. 1. Current density (solid line, right axis) and integrated luminescence intensity vs time (dotted line, left axis) of n-type GaP (doping density $10–20 \times 10^{17}$ cm^{-3}) during the first 1000 s of porous etching at 7 V in aqueous 0.5 M H_2SO_4 solution.

area. The branched structure forms a hemispherical domain, which grows isotropically ($t < 200$ s, Fig. 1). After some time the domains meet; this stabilises the active etching front and the anodic current becomes constant. From this point the porous layer, having a uniform thickness, grows in a direction perpendicular to the surface.

Surprisingly, light emission was observed during porous etching when the potential was sufficiently positive. Luminescence spectra were recorded every 60 s (using an exposure time of 60 s). In Fig. 1, the integrated luminescence intensity (I) in the range between 350 and 880 nm is plotted together with the current density as a function of time. Obviously, the luminescence is correlated with the anodic current; both increase in a similar way. From this and results shown below we conclude that the luminescence arises from the active etching area, i.e. the pore fronts. After 450 s the *recorded* luminescence intensity gradually starts to decrease, while the anodic current density remains constant. This is due to the growth of the porous layer, located between the light emitting area and the detector; photons are scattered and/or absorbed by the porous layer.

Fig. 2 shows a spectrum (a) which was recorded after 450 s while the current was constant but the porous layer was too thin to scatter photons significantly. Quite remarkably, a large fraction of the emitted photons have an energy close to and larger than the indirect bandgap (indicated by a dotted line in Fig. 2). This spectral distribution is quite different from that measured in a conventional photoluminescence experiment at ambient temperature [16,20]. Electroluminescence with peroxydisulfate, in which holes are injected into the valence band of GaP at negative potential, is shown in Fig. 2, spectrum c. This process is about 15 times more efficient than emission observed during porous etching. The broad peak at around 1.55 eV, also observed in cathodoluminescence [18] and photoluminescence at room temperature [16], is attributed to radiative recombination via a donor–acceptor pair in the bandgap [16,18]. However, there is a very striking additional contribution to the spectrum between 1.75 and 2.75 eV. Supra-bandgap emission is also observed in microporous silicon [21]. This broad emission in

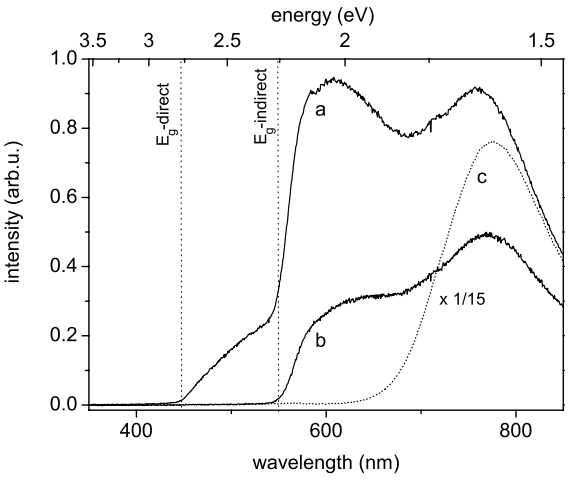

Fig. 2. Luminescence spectra of n-type GaP (doping density $10–20 \times 10^{17}$ cm^{-3}) after 450 s (a) and 10230 s (b) of porous etching at 7 V in aqueous 0.5 M H_2SO_4 solution. A luminescence spectrum (c) of n-type GaP (doping density $10–20 \times 10^{17}$ cm^{-3}) at negative potential in aqueous 20 mM $(NH_4)S_2O_8$/0.5 M H_2SO_4 solution is added for comparison.

the visible range can be excited either by light (photoluminescence) [21] or electrochemically [22]. The observation of only low-energy defect emission from our porous GaP in both photoluminescence [16] and hole-injection experiments shows that nanostructures cannot be responsible for the short-wavelength emission seen in Fig. 2.

The sharp decrease of the intensity with increasing energy at around 2.25 eV seen in spectrum a of Fig. 2 is related to the indirect bandgap of GaP at this energy. Due to this, the absorption mean free path of photons decreases from 250 μm at 2.2 eV to 0.3 μm at 2.8 eV [17]. Photons with a small diffusive absorption length can be recorded only if they are emitted in the direction of the detector. Photons with a very large diffusive absorption length can eventually reach the detector after being internally reflected inside the crystal or at the backside of the crystal. This explains the 'step' observed in the spectrum a (Fig. 2) at 2.25 eV. It is furthermore clear that after prolonged etching, the *detected* intensity decreased (Fig. 2, spectrum b) while the anodic current density remains constant. The supra-bandgap contribution is no longer recorded. This is due to scattering and absorption of the emitted photons by the porous

GaP layer. Photons with energy above the bandgap are strongly scattered and, eventually, absorbed. Photons with an energy below the bandgap are scattered only.

To obtain a better understanding of the origin of the luminescence, spectra were recorded while the potential of n-type GaP electrodes was scanned in the range in which porous etching occurs. We used GaP electrodes on which a thick porous layer ($L > 100$ μm) had been grown. This ensures that the relative increase in the thickness of the porous layer and thus additional absorption/scattering can be disregarded during the potential scan experiment. A scan speed of 25 mV/s was used and a spectrum was recorded every 20 s (with an exposure time of 20 s). We remark that the recorded spectra are similar to spectrum b of Fig. 2 and that the supra-bandgap contribution is absorbed. Under these conditions the luminescence spectrum did not depend on the applied potential. Experiments with a GaP electrode without a porous layer on the top showed that the ratio of the supra-bandgap and the sub-bandgap luminescence intensity did not depend on the applied potential. In Fig. 3 the current density (right axis) and the integrated luminescence intensity, between 550 and 880 nm (left axis), are plotted as a function of the applied potential. There is only a slight hysteresis in the current density when the potential is scanned to 7 V. The luminescence sets on at a potential 2 V more positive than the current density. The luminescence intensity increases rapidly with the applied potential.

It is known that at more positive potentials n-type GaP passivates in H_2SO_4 solution. The influence of passivation on the current density and the luminescence intensity is illustrated in Fig. 4. The current density in the forward scan shows a maximum at 7.8 V and decreases steeply above this potential as a result of passivation of the pore fronts by an oxide layer [19]. In the return scan, the current recovers slowly due to chemical dissolution of the oxide. This slow dissolution is responsible for the considerable hysteresis in the current density. The onset of the luminescence is at a higher potential than that of the current (Fig. 4). A considerable hysteresis is also observed in the intensity-potential curve. This again shows that the process of light emission is generated by current flow at the pore fronts.

A measure for the relative efficiency of the luminescence can be obtained by dividing the integrated intensity by the current density (insets of Figs. 3 and 4). Below ~4 V the current density is

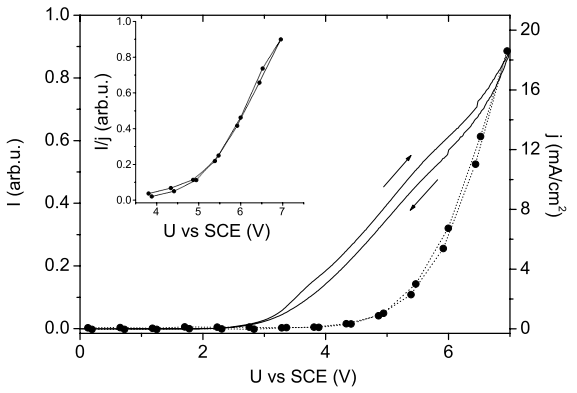

Fig. 3. Current density (solid line, right axis) and integrated luminescence intensity (dotted line, left axis) vs potential of porous n-type GaP (doping density $10–20 \times 10^{17}$ cm^{-3}). The measurement was done after 10^4 s of porous etching at 7 V in aqueous 0.5 M H_2SO_4 solution. The potential was scanned at a rate of 25 mV/s. Inset: Ratio of the current density and the integrated luminescence intensity vs potential.

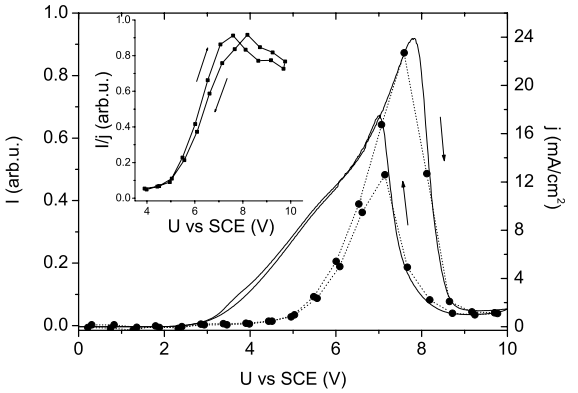

Fig. 4. Current density (solid line, right axis) and integrated luminescence intensity (dotted line, left axis) vs potential of porous n-type GaP (doping density $10–20 \times 10^{17}$ cm^{-3}). The measurement was done after 10^4 s of porous etching at 7 V in aqueous 0.5 M H_2SO_4 solution. The potential was scanned at a rate of 25 mV/s. Inset: Ratio of the current density and the integrated luminescence intensity vs potential.

close to zero and the efficiency cannot be estimated with a sufficient accuracy. Above 4 V the luminescence efficiency increases rapidly with increasing potential. The inset of Fig. 4 shows that the efficiency decreases slightly when a passivating oxide layer is formed ($U > 8$ V). The luminescence efficiency does not depend on the scan direction. This confirms that, with a thick porous layer, further growth of the layer during a potential scan does not significantly affect the recorded luminescence. Thus, Figs. 3 and 4 give a reliable representation of the potential dependence of the luminescence intensity.

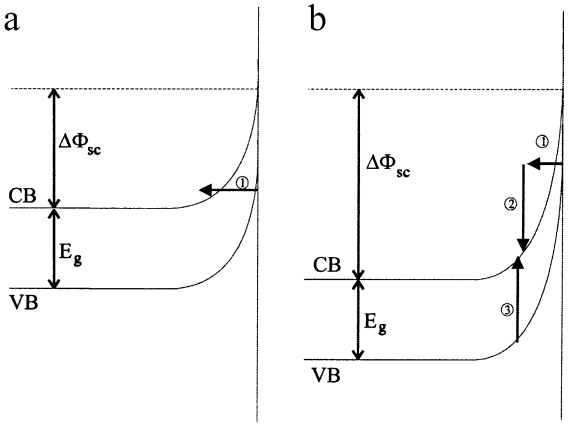

Fig. 5. Model for inter-band tunnelling (step 1) and impact ionisation (step 2 and 3) at different potential drops over the semiconductor ($\Delta\Phi_{sc}$), increasing from figure a to b.

4. Discussion

The electroluminescence observed during porous etching of n-type GaP at strongly positive potentials is clearly related to the anodic current originating from the pore fronts. Current flow in the reverse-biased junction must be due to "breakdown" of the depletion layer. This should depend on the electric field within the space-charge layer of the semiconductor. Impedance measurements by Erne et al. [2] both on porous and non-porous n-type GaP in H_2SO_4 solution showed that the depletion layer capacitance obeys the Mott–Schottky relation for potentials up to 9 V. This means that, in this range, a change in the applied potential results only in a change in the potential drop within the semiconductor. Since the flatband potential is known for the system (−1.2 V vs SCE [2]) the band bending can be determined for any value of the applied potential. At strong band bending empty states in the conduction band "overlap" with filled states at the top of the valence band at the surface. As a result, electrons can tunnel from the valence band to the conduction band (step 1, Fig. 5a). The electrons are detected as current in the external circuit. The holes generated in the valence band serve to oxidise the semiconductor, thus causing porous etching [2]. The onset of the current, shown in a semi-logarithmic plot in Fig. 6, corresponds to a band bending of 2.8 and 3.5 eV for the higher and lower doped electrodes, respectively. The relation between the current density due to inter-band tunnelling and the electric field, which was first derived by Zener [23] and extended for large bandgap semiconductors by McAfee et al. [24], is given by

$$j \sim E \cdot \exp\left[\alpha - \left(\frac{\beta}{E}\right)\right] \tag{1}$$

in which α is a parameter related to the semiconductor and E is, in our case, the electric field at the surface of the GaP electrode. The value of parameter β is given by the following equation:

$$\beta = \left(\frac{\pi^2}{eh}\right)(2m^*)^{1/2}E_g^{3/2} = 1.2 \times 10^{10}\ \text{V/m} \tag{2}$$

in which m^* is the effective electron mass [25] and E_g the bandgap. If it is assumed that the pore fronts are hemispherical, then the electric field at the surface of the pore fronts can be calculated [26]. By fitting the field dependence of the measured current, β-values of 5.3×10^9 and 3.2×10^9 V/m are found for the higher and the lower doped wafers, respectively. The reasonable agreement between the values of β calculated on the basis of a hemispherical pore front and the value predicted by theory (Eq. (2)) support a Zener-type mechanism for current and pore formation. Tunnelling of electrons from the valence band to the conduction band alone cannot explain light emission during anodic etching. While the hole concentration may be high, the electron concentration is extremely low due to the very high electric field.

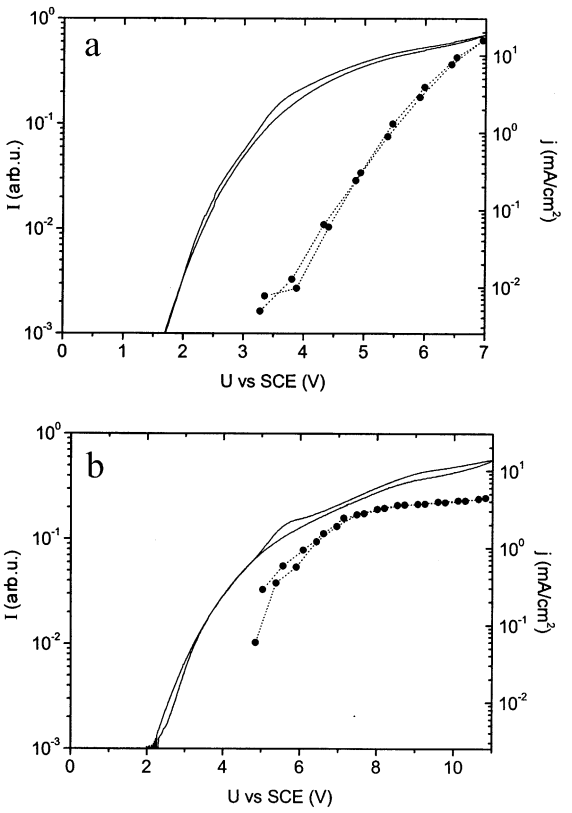

Fig. 6. Current density (solid line, right axis) and integrated luminescence intensity (dotted line, left axis) vs potential of porous n-type GaP with dopant density $10–20 \times 10^{17}$ cm^{-3} (a) and 7×10^{17} cm^{-3} (b). The measurement was done after 10^4 s of porous etching at 11 V in aqueous 0.5 M H_2SO_4 solution. The potential was scanned at a rate of 25 mV/s. (Fig. 6a—data from Fig. 3 in semi-logarithmic plot.)

The onset of luminescence is at a potential of about 2 V more positive than the onset of the current (Fig. 6). Electroluminescence has been observed in reverse-biased p–n junctions based on GaP [15,27–29] and the GaAsP [14] ternary system. The mechanism proposed for light emission in this case is impact ionisation [30]. A similar process is very likely also responsible for luminescence in our reverse biased n-type electrodes. Electrons injected into the conduction band are accelerated toward the bulk by the high electric field of the depletion layer. If the electron can gain more energy than the bandgap before it looses energy via an optical phonon, it can excite a valence band electron over the bandgap (steps 2 and 3 in Fig. 5b). The electron which is created by impact ionisation can in turn pick up energy from the field. This can give rise to an avalanche process with current multiplication [31]. Since the band bending in our case is rather low compared to that reported for p–n junctions [15], an avalanche process is unlikely. The threshold electric field for impact ionisation is, to a first approximation, given by $(3/2)E_g/(q \cdot \lambda)$ where λ is the optical phonon mean free path [32]; for GaP, λ is 3.0 nm [32] and thus the threshold field is $\sim 1 \times 10^9$ V/m. The electric field at the surface of a hemispherical pore is of this order of magnitude and impact ionisation can therefore be expected in our system. The probability of impact ionisation increases rapidly with increasing electric field at the surface [32]. This explains the increase in luminescence efficiency as the potential is raised (inset of Fig. 3). The electric field at the surface of the pore fronts decreases when passivation occurs; a part of the applied potential drops over the oxide layer. This reduces the efficiency of the luminescence, as is observed in the inset of Fig. 4.

Hole-injection from an oxidising agent under forward-bias (Fig. 2, spectrum c) and optical excitation at room temperature [16] give a broad emission band that is similar to the band at about 770 nm observed at strongly positive potentials in this work (Fig. 2). This emission can be attributed to radiative recombination of thermalised electrons and holes via defect states [16]; in this case the charge carriers are in quasi equilibrium. In contrast, the high-energy contribution of the observed spectrum with a significant supra-bandgap shoulder ($1.75 \text{ eV} < \lambda < 2.75$ eV) must be related to the relaxation of hot charge carriers formed at severe band bending ($U > 4$ V). Similar features have been observed in strongly reverse-biased GaP [15,27–29] and ternary GaAsP [14] p–n junctions. Very localised emission spots were observed, occurring at imperfections in the junction. In the present work emission is triggered at the pore fronts where the electric field is greatly enhanced; as a result, luminescence is observed at considerably more modest bias than that required for a good-quality p–n junction. The emission sets on at the direct bandgap of GaP (Fig. 2, spectrum a), as observed in reference [14]. The supra-bandgap

emission can be due to recombination of holes with electrons in the conduction band minimum that corresponds to the first direct bandgap (the Γ-point [33]). We conjecture that under high field conditions this conduction band minimum can be populated [31]. Radiative recombination between the conduction band minimum at the X-point and the maximum of the valence band is less efficient [14]. The increase of the luminescence intensity from 2.75 eV can also be related to the diffusive absorption length, which strongly increases with decreasing energy.

It is clear from the above results and discussion that generation of minority carriers, which is essential for light emission, is made possible by the very strong electric field of the depletion layer at the pore fronts. It is also clear that, as in the case of the strongly reverse-biased p–n junctions, radiative recombination must occur within the space-charge layer.

These results therefore show that during porous etching of n-type GaP at strongly positive potentials a light source, consisting of a collection of emitting sites, is created at the interface between porous and non-porous GaP. This source, which has a broad spectrum in the visible range, moves with the interface as the porous layer thickens; it can therefore be used to study light scattering in this strongly scattering porous medium [34].

Acknowledgements

The work described here was supported by the Council of Chemical Sciences (CW) and Foundation for Fundamental Research on Matter (FOM) with financial aid from the Netherlands Organisation for Scientific Research (NWO).

References

[1] J.J. Kelly, D. Vanmaekelbergh, Porous etched semiconductors; formation and characterization, in: The Electrochemistry of Nanomaterials, Weinheim, Germany, 2001 (Chapter 4).
[2] B.H. Erne, D. Vanmaekelbergh, J.J. Kelly, J. Electrochem. Soc. 143 (1996) 305.
[3] T. Takizawa, S. Arai, M. Nakahara, Jpn. J. Appl. Phys. Part 2 Lett. 33 (1994) L643.
[4] S. Langa, I.M. Tiginyanu, J. Carstensen, M. Christophersen, H. Foll, Electrochem. Solid State Lett. 3 (2000) 514.
[5] P. Schmuki, J. Fraser, C.M. Vitus, M.J. Graham, H.S. Isaacs, J. Electrochem. Soc. 143 (1996) 3316.
[6] G. Oskam, A. Natarajan, P.C. Searson, F.M. Ross, Appl. Surf. Sci. 119 (1997) 160.
[7] X.L. Li, Y.W. Kim, P.W. Bohn, I. Adesida, Appl. Phys. Lett. 80 (2002) 980.
[8] F. Schuurmans, University of Amsterdam, 1999.
[9] F.J.P. Schuurmans, D. Vanmaekelbergh, J. van de Lagemaat, A. Lagendijk, Science 284 (1999) 141.
[10] F.J.P. Schuurmans, M. Megens, D. Vanmaekelbergh, A. Lagendijk, Phys. Rev. Lett. 83 (1999) 2183.
[11] P.M. Johnson, B.P.J. Bret, J. Gómez Rivas, J.J. Kelly, A. Lagendijk, Phys. Rev. Lett. 89 (2002) 243901.
[12] E. Kikuno, M. Amiotti, T. Takizawa, S. Arai, Jpn. J. Appl. Phys., Part 1-Regular Papers Short Notes and Review Papers 34 (1995) 177.
[13] B.H. Erne, D. Vanmaekelbergh, J.J. Kelly, Adv. Mater. 7 (1995) 739.
[14] M. Pilkuhn, H. Rupprecht, J. Appl. Phys. 36 (1965) 684.
[15] M. Gershenzon, R.M. Mikulyak, J. Appl. Phys. 32 (1961) 1338.
[16] B. Smandek, H. Gerischer, Electrochim. Acta 30 (1985) 1101.
[17] D.E. Aspnes, A.A. Studna, Phys. Rev. B: Condens. Matter 27 (1983) 985.
[18] M.A. Stevens-Kalceff, I.M. Tiginyanu, S. Langa, H. Foll, H.L. Hartnagel, J. Appl. Phys. 89 (2001) 2560.
[19] R.W. Tjerkstra, J. Gómez Rivas, D. Vanmaekelbergh, J.J. Kelly, Electrochem. Solid State Lett. 5 (2002) G32.
[20] A. Meijerink, A.A. Bol, J.J. Kelly, Appl. Phys. Lett. 69 (1996) 2801.
[21] A.G. Cullis, L.T. Canham, P.D.J. Calcott, J. Appl. Phys. 82 (1997) 909.
[22] E.S. Kooij, A.R. Rama, J.J. Kelly, Surf. Sci. 370 (1997) 125.
[23] C. Zener, Proc. Royal Soc. (London) A 145 (1934) 523.
[24] K.B. McAfee, E.J. Ryder, W. Shockley, M. Sparks, Phys. Rev. 83 (1951) 650.
[25] G. Burns, Solid State Physics International Edition Orlando, Florida, 1985.
[26] X.G. Zhang, J. Electrochem. Soc. 138 (1991) 3750.
[27] G.A. Wolff, R.A. Hebert, J.D. Broder, Phys. Rev. 100 (1955) 1144.
[28] F.G. Ullman, Nature 190 (1961) 161.
[29] H.C. Gorton, J.M. Swartz, C.S. Peet, Nature 188 (1960) 303.
[30] J.I. Pankove, Optical Processes in Semiconductors, New York, NY, 1975.
[31] S.M. Sze, Physics of Semiconductor Devices, second ed., Murray Hill, N. Jersey, 1981.
[32] Y. Okuto, C.R. Crowell, Phys. Rev. B 6 (1972) 3076.
[33] J.R. Chelikowsky, M.L. Cohen, Phys. Rev. B 14 (1976) 556.
[34] A.F. van Driel, in press.